5th ECPMG Delft · 2024

Proceedings of the 5th ECPMG 2024
5th European Conference on Physical Modelling in Geotechnics
2-4 October 2024, Delft, the Netherlands

Nailing Reinforcement Mechanism for Soil Slopes with Dual Structure under Drawdown Condition

Yueyan. Hao
Ga. Zhang
Department of Hydraulic Engineering, Tsinghua University, 100084, Beijing, China,
zhangga@tsinghua.edu.cn

ABSTRACT: Water level variation is a significant threaten to the slope stability. Soil nails are commonly used in slope reinforcement. However, the reinforcing mechanism of soil nails on heterogenous slopes has not been adequately investigated. In this study, centrifuge model tests were conducted on a typical heterogeneous slope with dual structure under drawdown condition. The slope model is made up of loess and sand layers with different soil nail layouts. Full field displacement of the slope was obtained using image-based measurement. The test results show that the nails increase the stability level and reduce the deformation of heterogeneous slopes. The slip surface of the slope is remarkably affected by the nails especially the shape and depth. The reinforced slope exhibits a downward progressive failure from the slope top. The failure mechanism is that the drawdown produces deformation localization which further leads to local failure. The nail-soil interaction makes the deformation distribution more uniform so that the degree of deformation localization decreases. As a result, the safety level of the heterogeneous slope is enhanced.

1 INTRODUTION

Drawdown poses a significant threat to the stability of soil slopes in reservoir areas. Soil nails are a widely used and effective method for reinforcement (Turner et al., 2005). Extensive research has validated their reinforcement efficacy under diverse conditions such as seepage, earthquakes, and loading (Deepa et al., 2009; Yang et al., 2020; Zhang et al., 2014).

Centrifuge model test creates a hypergravity field through centrifugal force with stress conditions equal to the prototype in a scaled model. By modifying the apparatus, various seepage conditions can be simulated in the experiment. Consequently, centrifuge model testing stands as a principal slope stability analysis method. Rotte et al. (2012) investigated the impact of soil nail inclination angle and slope material on the stability of soil nail-reinforced slopes under seepage conditions through centrifuge model tests. Zhang and Jin (2016) delved into the influence of soil nail length on the failure mechanism of soil nail-reinforced slopes under drawdown conditions.

However, existing studies primarily focus on homogeneous slopes, while natural slopes are predominantly heterogeneous. Heterogeneous structures have a significant influence on slope's response to drawdown (Wang et al., 2012). For example, dual structure causes the slope deformation and failure exhibit distinct characteristics from the homogeneous condition (Hao et al., 2022).

Therefore, it becomes imperative to explore the reinforcement mechanism of soil nails for heterogeneous slopes. This study specifically selects a dual structural slope containing sand and loess and investigates its nail reinforcement mechanism under drawdown condition through centrifuge model tests. Measurements of soil slope displacement are conducted, and deformation and failure modes are analysed, which reflect the characteristics of dual structure and reveal the reinforcement mechanism of soil nails.

2 TESTS

2.1 Test program

Centrifuge model test is chosen as the main research method. To analyse the soil nail reinforcement characteristics on the slope with dual structure under drawdown, slope model with loess and sand layers is chosen. The deformation and failure of two same slope models with and without soil nails reinforcement in the loess layer under drawdown condition are simulated in the tests. Each tests encompass identical impoundment and drawdown procedures.

2.2 Equipment

The centrifuge model tests were conducted on the geotechnical centrifuge in Tsinghua University with a maximum acceleration of 250 g. The centrifuge operates on the principle of rotating a model to simulate hypergravity via centripetal acceleration. A 600 mm long, 200 mm wide, and 500 mm high model box is installed on centrifuge to contain model. A 40 mm thick plexiglass is affixed to one lateral side of model box for observation.

To produce water level variations, a water level simulation system was employed in tests (Luo and Zhang, 2016). The model box has a water pipe inside to add water and a drainage hole at the bottom to release water. A pore water pressure transducer is installed at the bottom of the model box, which can monitor water level and control the adding or releasing of water.

2.3 Model

Sand and loess are chosen due to their distinct differences in strength, deformation, and permeability characteristics, resulting in a notable deviation from homogeneous slopes. The sand is Fujian standard sand with dry density of 1.55 g/cm^3 and moisture content of 17%. Its average soil particle size, d_{60} particle size and d_{10} particle size are 0.45mm, 0.5mm and 0.29mm, respectively. The loess is silty loess with dry density of 1.5 g/cm^3 and moisture content of 17%. The liquid and plastic limits of the soil are 31% and 17%, respectively.

The slopes are 0.75:1 and 240 mm in height. The thickness of each layer is 120 mm. (Fig. 1). When preparing the model, the soil with specified water content is compacted to the designed dry density in the model container with a thickness of 40 mm. The top of each layer is scraped to enhance the bonding with the overlying layer. After completing all layers, the shape of the slope is carved out.

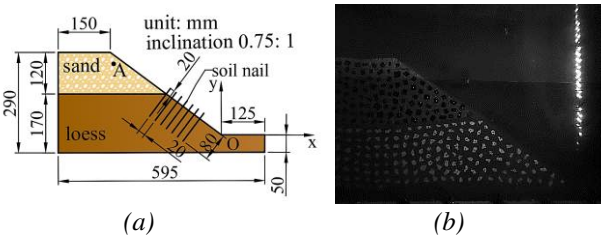

(a) (b)

Figure 1. Nail reinforced slope model. (a) Diagrammatic sketch; (b) Photograph.

After the slope model is made, soil nails are inserted at 2cm intervals horizontally and along the slope. These nails, simulated by steel wires, are placed in seven rows atop the loess layer. Each steel wire measures 0.7mm in diameter and 10cm in length, penetrating the soil slope vertically to a depth of 8cm.

2.4 Measurement

Image acquisition and displacement measurement system is utilized to capture image series of the slope model from the plexiglass side of the model box during tests. Displacement of points on the slope is measured using a correlation-based algorithm (Zhang et al., 2009). Numerous small and irregular foams are affixed to the soil slope surface with pins behind the plexiglass, aiming to enhance grayscale differences and improve displacement measurement accuracy to 0.03 mm at model scale during the tests.

A Cartesian coordinate system is established with the toe of the slope as the origin, defining the positive x-axis and y-axis directions as rightward and upward, respectively (Fig. 1 (a)). Positive values for horizontal and vertical displacements are defined in the rightward and downward directions, respectively.

According to the similarity law of the centrifuge model test, the size, water level and displacement in the model scale can be transformed to the prototype scale by multiplying acceleration. Stress and strain in the model scale are equivalent to those in the prototype scale. Rates of drawdown and seepage in the model scale can be converted to the prototype scale by dividing the centrifugal acceleration, while time in the model scale is transformed to the prototype scale by multiplying the square of the acceleration. It is crucial to emphasize that all measurement results presented in this paper are in the model scale.

2.5 Test Procedure

All the tests are conducted using the following steps:

(1) The centrifugal acceleration is increased to 5 g, 10 g, …, 50 g. In each loading stage, the centrifugal acceleration is kept constant for a while until the slope settlement.

(2) There is no water in the model box initially. The water level is raised from 0mm to 200 mm from the slope toe by five stages, 40 mm each. In each impoundment stage, the water level is maintained stable for 10 minutes to let the water fully penetrate in the slope and the slope settlement become stable. After the impoundment is finished, the slope is stabilized for 20 minutes.

(3) Open the drainage hole and the water level is decreased at one time to slope toe at a roughly uniform speed. The drawdown process is shown in Fig. 2. The vertical displacement of typical point A, whose position is shown in Fig. 1, starts to increase fast at a certain moment (Fig. 2).

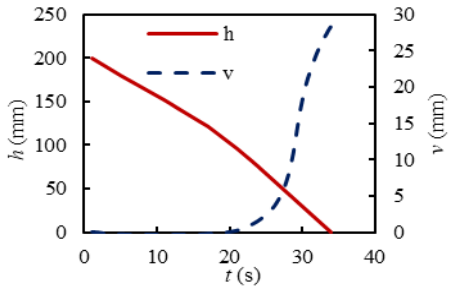

Figure 2. Drawdown history of the two slopes. t, time; h, water level; v, vertical displacement of point A.

3 FAILURE BEHAVIOR

3.1 Slip surface

Fig. 3 shows the photographs of the two slopes after landslide. Through observing the image series of slope failure and measuring full field displacement, slip surface is determined at the positions with sudden change in displacement distribution after slope failure and can be clearly distinguished from the image.

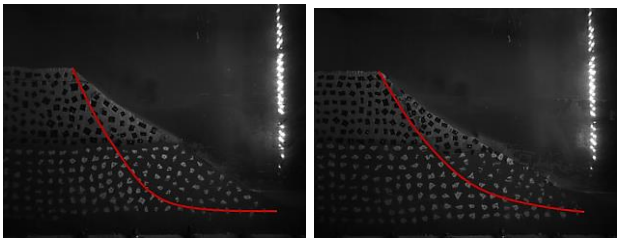

(a) *(b)*

Figure 3.Slopes after failure. Red line, slip surface. (a) Reinforced slope; (b) Unreinforced slope.

Failure occurs in almost the same range of height of the two slopes and both runs through the slopes. The slip surface in the sand layer is nearly a straight line while that in the loess layer looks like circular arc. This indicates that the sand layer slides translationally and the loess layer slides rotationally. The interaction between the two layers is prominent near the junction.

Soil nails changes the shape of slip surface mainly in loess layer. In the reinforced slope, the slip surface in the loess layer generally lies deeper than the soil nails, indicating a bypassing-nails failure mechanism. Moreover, the reinforced slope exhibits a deeper slip surface compared to the unreinforced slope, with the difference being more pronounced near the bottom. Consequently, soil nails transmit the impact of drawdown to a larger range of the slope.

3.2 Failure Process

The reinforced and unreinforced slopes both exhibit progressive failure. Point couple analysis is used to determine the local failure moment along the slip surface. A point couple is a pair of points on opposite sides of the slip surface.

Fig. 4 shows relative displacement history of point couples in the direction tangential to the slip surface. The increase rate of tangential relative displacement remains quite small in the initial stage and significantly escalates at a water level. It can be deduced that substantial relative tangential displacement is triggered by local failure. Thus, the local failure is determined by the intersection of the tangents of the historical curve before and after the inflection point.

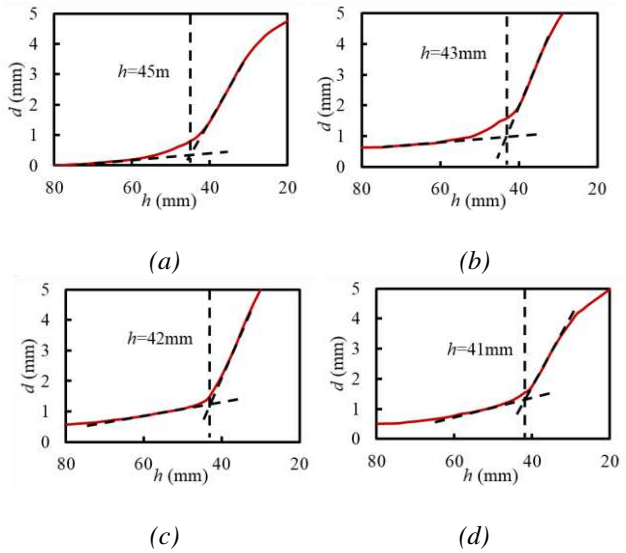

(a) *(b)*

(c) *(d)*

Figure 4. History of relative displacement of point couples along slip surface of reinforced slope. (a) y=203mm; (b) y=153mm; (c) y=67mm; (d) y=13mm. h, water level.

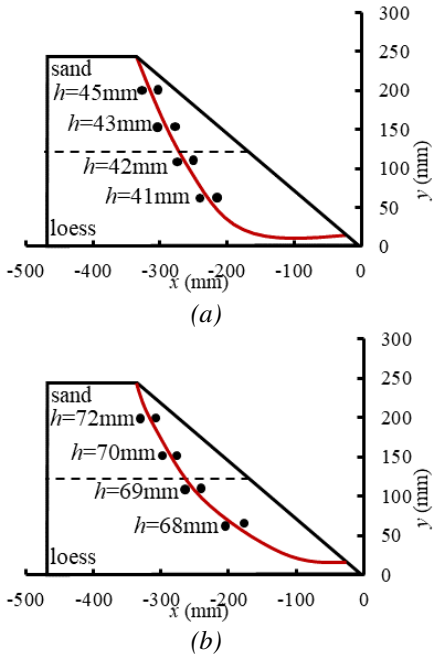

(a)

(b)

Figure 5. Point pair locations and failure progress of slopes. (a) Reinforced slope; (b) Unreinforced slope.

The local failure sequentially occurs from top to bottom of the slope. The development of slip surface in both slopes undergoes a comparable range of water level fluctuations. It can be concluded that soil nails do not alter the failure sequence but rather postpone the onset of failure. Thus, soil nails increase the safety limit of the slope.

4 MECHANISM ANALYSIS

4.1 Failure Mechanism

Serval points were selected at a certain height in the slope and track their horizontal displacement from the beginning of drawdown. The horizontal displacement of these points reflects the slope's distribution at that height. Fig. 6 shows horizontal distribution of horizontal displacement of a certain height at various water levels prior to the failure of the loess layer in the two slopes. The coordinates in Fig. 6 correspond to the coordinate system in Fig. 1 (a). As water drawdown, the horizontal displacement in the interior part of the slopes remains minimal while, in the outer part, the horizontal displacement is much larger. Such uneven displacement development signifies local deformation in the slopes. Besides, inflection points gradually emerge on the distribution curves, marking the positions of the most significant local deformation. These inflection points coincidentally lie on the locations forming slip surfaces. Local failure of the slopes may have relations with the uneven displacement distribution and local deformation development.

Close analysis shows that in the reinforced slope, the development of horizontal displacement lags behind that of the unreinforced slope. This result indicates that soil nails hinder the development of displacement.

The maximum shear strain is selected as the specific indicator to study on the relationship between deformation localization and slope failure. It is calculated by using a analysis scheme similar to the finite element method on a square element with a side length of 6 mm whose node displacements are measured using image analysis.

Fig. 7 and Fig. 8 show horizontal distributions of maximum shear strain at different layers of the two slopes before slope failure. The lowest water level in each figure is 3 mm higher than that of local failure. Initially, the maximum shear strain is uniformly small, gradually increasing during water drawdown. However, such increase exhibits diverse progress in different locations. At each elevation, a specific area experiences a notably faster rise in maximum shear strain, reaching significant magnitudes. Conversely, beyond this, the increase is maintaining small the entire process.

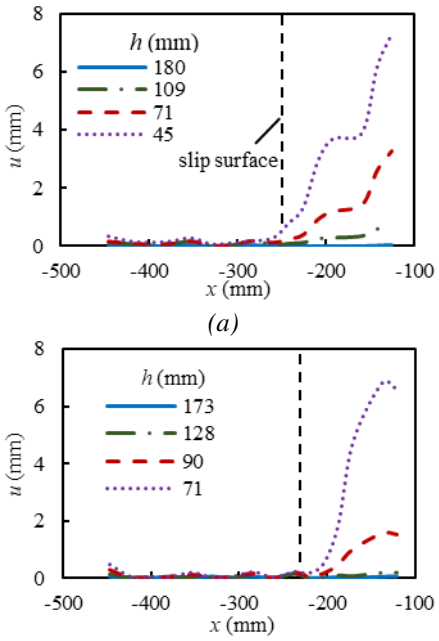

Figure 6. Horizontal distribution of horizontal displacement of slopes at y=67 mm; (a) Reinforced slope; (b) Unreinforced slope. u, horizontal displacement; h, water level.

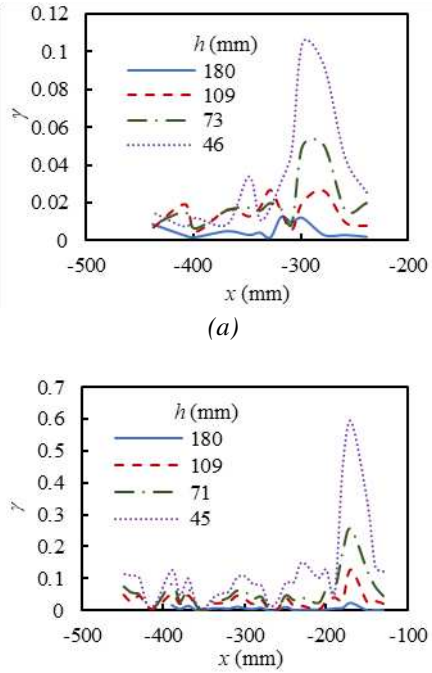

Figure 7. Horizontal distribution of maximum shear strain of reinforced slope. (a) y=160mm; (b) y=67mm. γ, maximum shear strain.

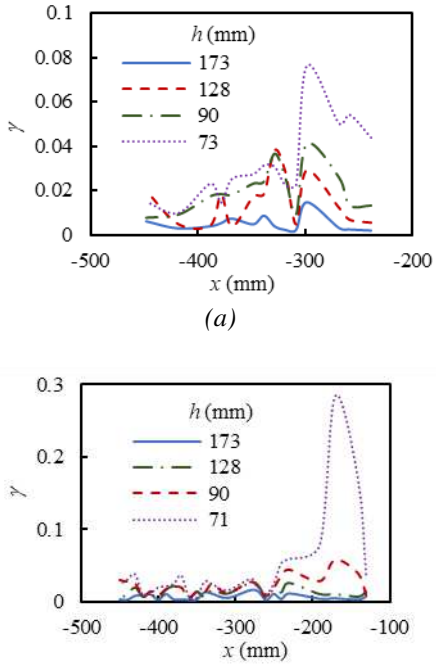

Figure 8. Horizontal distribution of maximum shear strain of unreinforced slope. (a) y=160mm; (b) y=67mm. γ, maximum shear strain.

Thus, the horizontal distribution curve of maximum shear strain exhibits a peak. This peak region corresponds to the segment with the most pronounced deformation localization. Comparing the location of local slip surface to the peak area, it becomes evident that local failure ultimately occurs in the peak area. Hence, the development of deformation localization causes local failure.

4.2 Reinforcement Mechanism

Fig. 9 shows the maximum shear strain development progress of typical points of reinforced and unreinforced slopes. These points correspond to the peaks of the maximum shear strain distribution curves presented in Figs. 7-8 and are considered representative of deformation localization at the same elevation. This is because, as water drawdown, in a certain elevation, the maximum shear strain value continues to increase and the range of the deformation localization area also keeps expanding, but the maximum shear strain distribution curves basically keep stable shape and just proportional amplify. Thus, the maximum shear strain development process everywhere is similar and maximum shear strain development of the whole slope at this elevation can be inferred from that at peak position.

The maximum shear strain of each position develops as drawdown and increase rapidly after a certain moment, showing inflection points on the time history curve. The inflection point on the curve of the reinforced slope is not as sharp as that in unreinforced slope and appears later. After the inflection point, the maximum shear strain in reinforced slope increases much slower than that in unreinforced slope and the final maximum shear strain in reinforced slope is much smaller. It can be concluded that the soil nails delay the development of deformation localization and improve the stability of slope.

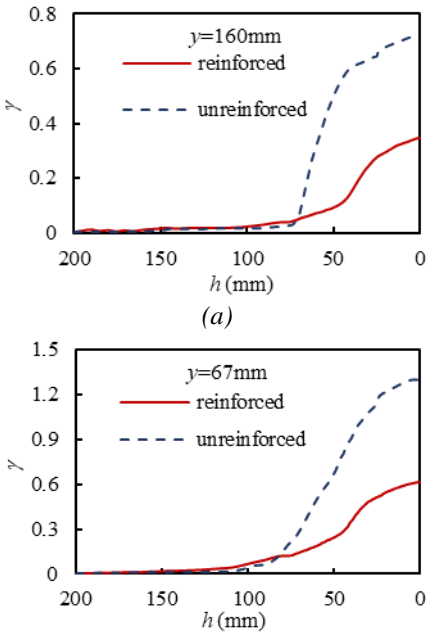

Figure 9. History of maximum shear strain of typical points of different slopes. γ, maximum shear strain; h, water level.

Fig. 10 compares the distribution of the maximum shear strain at the same elevation in two soil slopes just before local failure. The reinforced slope exhibits a broader range of deformation localization. And in deformation localization area, the maximum shear strain is also higher than unreinforced slope. It can be concluded that the soil nails cause the slope deformation distribution to become more uniform and enhancing the slope stability. This also explains why the soil nails can improve the safety limit of dual structure slope.

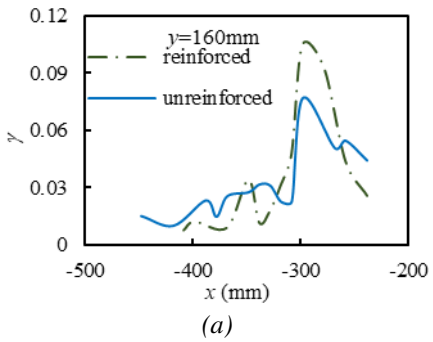

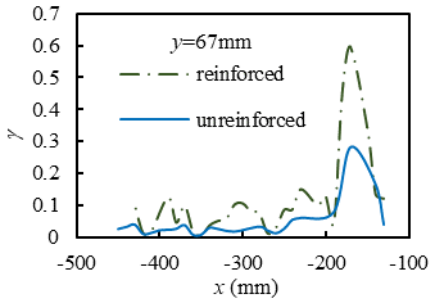

(b)

Figure 10. Horizontal distributions of maximum shear strain in different slopes when water level is 3mm before local failure. (a) y=160mm; (b) y=67mm; γ, maximum shear strain.

5 CONCLUSION

This study carries out centrifuge model tests to explore the soil nail reinforcement mechanism on dual structure slope with sand and loess. Conclusions are drawn as follows:

(1) Drawdown leads to significant progressive failure of the dual structure slope from the top to the bottom. The sand layer mainly undergoes translational sliding, while the loess layer slides rotationally.

(2) Soil nails increase the stability level and reduce the deformation of the slope. Soil nails do not change the failure pattern of the slope, but cause the slip surface deeper.

(3) The failure mechanism is that the drawdown produces deformation localization which further leads to local failure.

(4) The reinforcement mechanism of soil nails is that the soil nails cause the slope deformation distribution more uniform and thus reduce the extent of deformation localization of the slope.

ACKNOWLEDGEMENTS

The authors are grateful for the financial support by Beijing Natural Science Foundation (No. QY23146) and National Key R&D Program of China (No. 2023YFC3007001).

REFERENCES

Deepa, V., & Viswanadham, B. V. S. (2009). Centrifuge model tests on soil-nailed slopes subjected to seepage. *Proceedings of the Institution of Civil Engineers-Ground Improvement, 162(3),* 133-144.

Hao, Y., Luo, F., & Zhang, G. (2022). Centrifuge Modeling of Soil Slopes with Dual Structure Under Drawdown Conditions. In *International Conference of the International Association for Computer Methods and Advances in Geomechanics* (pp. 433-440). Cham: Springer International Publishing.

Luo, F., & Zhang, G. (2016). Progressive failure behavior of cohesive soil slopes under water drawdown conditions. *Environmental Earth Sciences, 75,* 1-12.

Rotte, V. M., & Viswanadham, B. V. S. (2012). Performance of 2V: 1H slopes with and without soil-nails subjected to seepage: Centrifuge study. In *GeoCongress 2012: State of the Art and Practice in Geotechnical Engineering* (pp. 643-652).

Turner, J. P., & Jensen, W. G. (2005). Landslide stabilization using soil nail and mechanically stabilized earth walls: case study. *Journal of Geotechnical and Geoenvironmental Engineering, 131(2),* 141-150.

Yang, T., Zou, J. F., & Pan, Q. J. (2020). Three-dimensional seismic stability of slopes reinforced by soil nails. *Computers and Geotechnics, 127,* 103768.

Zhang, G., Cao, J., & Wang, L. (2014). Failure behavior and mechanism of slopes reinforced using soil nail wall under various loading conditions. *Soils and Foundations, 54(6),* 1175-1187.

Zhang, G., Hu, Y., & Zhang, J. M. (2009). New image analysis-based displacement-measurement system for geotechnical centrifuge modeling tests. *Measurement, 42(1),* 87-96.

Zhang, G, & Jin, H. L. (2016). Failure behavior of soil nailing-reinforced slopes under drawdown conditions. *Rock and Soil Mechanics, 37,* 137-143 (in Chinese).

Wang, J. J., Zhang, H. P., Zhang, L., & Liang, Y. (2012). Experimental study on heterogeneous slope responses to drawdown. *Engineering geology, 147,* 52-56.